24th COBEM - 2017

24th ABCM International Congress of Mechanical Engineering
December 3-8, 2017, Curitiba, PR, Brazil

COBEM-2017-0434
NONLINEAR DYNAMICS OF A ROTATING SYSTEM CONSIDERING CONTACT WITH A SHAPE MEMORY ALLOY COATED STATOR

Rodrigo Veronese Moreira
Alberto Paiva
Universidade Federal Fluminense
420 Trabalhadores Av. – Volta Redonda, RJ – Brazil – 27.255-250
rodrigo_vr@msn.com
paiva.ufrj@gmail.com

Abstract: *Rotating machines have been used in large scale since the first industrial revolution; thus, for more than a hundred years, dynamical models have been developed and refined in order to describe such systems behavior. A very common phenomenon in rotating dynamics is the intermittent contact between rotor and bearing, which induces undesirable behaviors that may both compromise endurance and prevent the system from working properly. In the last decades, the development of intelligent materials has brought up new possibilities to avoid such inconvenience, taking advantage of particular properties of this kind of materials, for instance: intrinsic energy dissipation and adaptability. This work presents a rotating system model based upon the Jeffcott rotor with four degrees of freedom, being two of them related to the rotor, while the other two refer to the bearing. The bearing inner surface, which is subjected to contact, is coated with Shape Memory Alloy (SMA), whose behavior is described by a first-order phase transition polynomial constitutive model. The SMA coating together with the intermittent contact enable nonlinear characteristics, which lead to a vast richness of dynamical behavior including chaos. Furthermore, the system dynamical response depends on this SMA coating layer temperature, which affects the material behavior (stiffness) and directly influences the impact forces. This element temperature is subjected to two competing phenomena: heating deriving from friction during impact and cooling as a result of convection caused by the interaction with the surrounding environment.*

Keywords: *Jeffcott rotor, shape memory alloys, Falk model, nonlinear dynamics, chaos.*

1. INTRODUCTION

Rotating systems usually present a very complex dynamical response, especially when intermittent contact occurs between rotor and stator. The first rotor models (Rankine, 1869; Jeffcott, 1919) did not consider any interaction with adjacent parts. As more refined models considering contact and friction were developed and solved by numerical methods, interesting dynamical behaviors were observed, such as nonlinearities and chaos (Choy and Padovan, 1987; Muszynska and Goldman, 1995). Nowadays, this topic is still of great interest, as recent authors have been studying the contact phenomena by different approaches (Edwards *et al.* 1999; Al-Beodoor, 2000; Popprath and Ecker, 2007; Chávez and Wiercigroch, 2013; Lahriri and Santos, 2013; Varney and Green, 2015; Fonseca *et al.* 2016). Recently, with the expanding SMA exploration (Birman, 1996; Paiva and Savi, 2006; Lagoudas, 2008, Cisse *et al.* 2016), new possibilities have arisen for nonlinear dynamic systems (Bernardini and Rega, 2010; Savi, 2015), including nonsmooth systems (Santos and Savi, 2009; Sitnikova *et al.* 2010) and rotor dynamics applications (Silva *et al.* 2013).

The dynamical model presented in this work deals with a 4-degree of freedom (DOF) rotor system consisting of a planar Jeffcott rotor and a stator, assuming 2 DOF each. The stator inner surface is coated with an SMA layer and is subjected to intermittent contact and friction with the rotor. The SMA behavior is based on the polynomial model proposed by Falk (Falk, 1980; Falk, 1983).

The contact forces between rotor and stator are affected by the SMA layer mechanical behavior, which depends on its temperature. On the other hand, the SMA layer temperature is affected by the contact forces themselves (inducing heating due to friction) and by the interaction with the surrounding environment (inducing cooling due to convection). Since the SMA temperature is calculated considering these two competing phenomena, it incorporates one more DOF in the mathematical formulation.

The nonlinear system characteristics result from both the intermittent contact possibility and the nonlinear temperature-dependent SMA layer behavior. These features lead to a vast richness of dynamical behavior including chaotic responses. This work aims to analyze such dynamical responses and investigate the influence of the convective coefficient over the system dynamics.

2. MATHEMATICAL MODELING

The dynamical model consists of a Jeffcott rotor with mass m_r and a stator with mass m_s as shown in Fig. 1. The stator presents an SMA layer coating its inner surface, which is subjected to contact with the rotor. Stiffness and damping associated with rotor deflection and stator displacement are represented by "rotor supports" and "stator supports", respectively. Stator and rotor supports stiffness are given by k_r and k_s, while damping constants are given by c_r and c_s, respectively. The system excitation is a result of the rotor unbalancing, which is represented by an eccentric center of gravity M shifted from its geometric center O by a distance e. Rotor angular velocity is represented by Ω, while the gap between rotor and stator is given by γ.

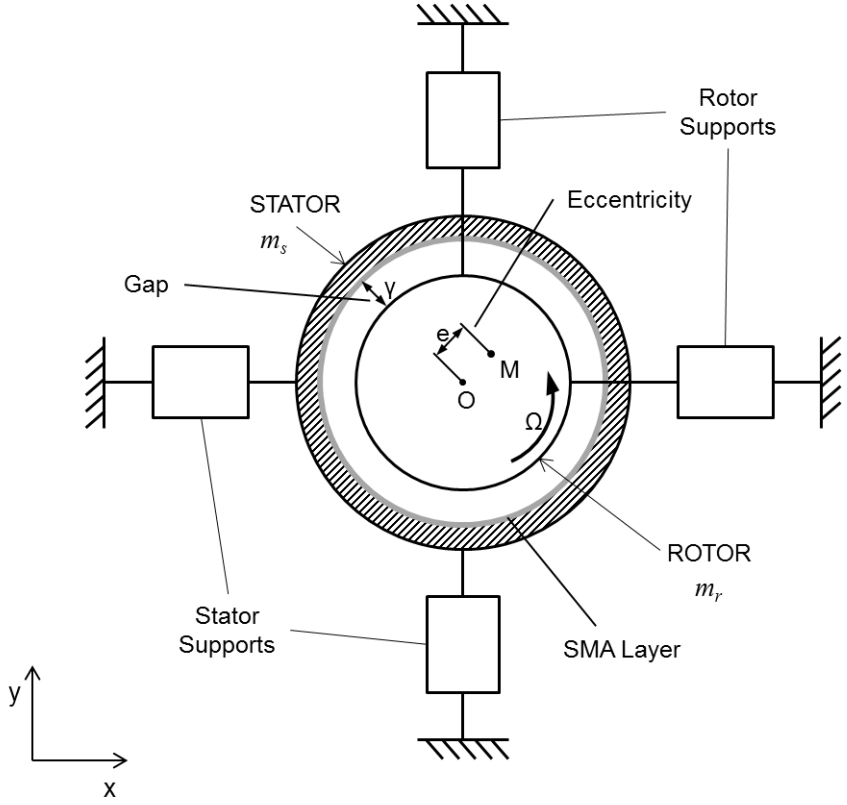

Figure 1. Rotor-stator model.

Equation (1) presents the equations of motion, where acceleration due to gravity is given by g. Rotor displacements in x and y directions are given by x_r and y_r, respectively; while stator displacements in x and y directions are given by x_s and y_s, respectively. The contact forces are given in x and y directions by F_{Cx} and F_{Cy}, respectively. Regarding contact, it occurs every time the modulus of the relative displacement between rotor and stator $|\underline{r}_{sr}|$ exceeds the gap γ, as presented in Eq. (2). Contact forces concerning the SMA layer are presented by Eq. (3) for normal and tangential directions and are represented by F_{Cn} and F_{Ct}, respectively. Friction coefficient is represented by μ. The SMA behavior is based on the polynomial model proposed by Falk (1980), which is described as a function of the indentation δ, defined as $\delta = |\underline{r}_{sr}| - \gamma$ for contact conditions. The constants A, B and C are related to the original Falk parameters and stator geometry. T_l is the SMA layer temperature, while T_A and T_M represent the triggering transformation temperatures for austenitic and martensitic phases, respectively. Eq. (4) presents the contact forces decomposed in x and y directions, respectively.

The SMA layer temperature evolution is considered in Eq. (5), which establishes its temperature rate of change as a function of contact forces and convective phenomena. The ambient temperature is given by T_{amb}, while the convection coefficient is represented by h. Rotor radius is represented by r_r and λ is the fraction of heat stemming from friction that contributes to the SMA internal energy increase. The remaining constants, related to the SMA layer are: mass m_l, specific heat c_l and convection area A_l.

The whole set of equations is numerically solved using Runge-Kutta method.

$$
\begin{aligned}
&m_r\ddot{x}_r + c_r\dot{x}_r + k_r x_r = m_r e\Omega^2\cos(\Omega t) + F_{Cx}\\
&m_r\ddot{y}_r + c_r\dot{y}_r + k_r y_r = m_r e\Omega^2\sin(\Omega t) + F_{Cy} - m_r g\\
&m_s\ddot{x}_s + c_s\dot{x}_s + k_s x_s = -F_{Cx}\\
&m_s\ddot{y}_s + c_s\dot{y}_s + k_s y_s = -F_{Cy} - m_s g
\end{aligned}
\tag{1}
$$

$$
\begin{aligned}
&|\underline{r}_{sr}| < \gamma \rightarrow \text{Without contact}\\
&|\underline{r}_{sr}| \geq \gamma \rightarrow \text{With contact}
\end{aligned}
\tag{2}
$$

$$
\begin{aligned}
&F_{Cn} = A(T_l - T_M)\delta - B\delta^3 + \frac{C}{(T_A - T_M)}\delta^5\\
&F_{Ct} = \mu F_{Cn}
\end{aligned}
\tag{3}
$$

$$
\begin{aligned}
&F_{Cx} = F_{Cn}\frac{1}{|\underline{r}_{sr}|}\left[-(x_r - x_s) + \mu(y_r - y_s)\right]\\
&F_{Cy} = F_{Cn}\frac{1}{|\underline{r}_{sr}|}\left[-(y_r - y_s) - \mu(x_r - x_s)\right]
\end{aligned}
\tag{4}
$$

$$
\dot{T}_l = \frac{1}{m_l c_l}\left[\lambda F_{Ct} r_r \Omega - hA_l(T_l - T_{amb})\right]
\tag{5}
$$

3. RESULTS AND DISCUSSION

This section presents the results associated to the dynamical system described by Fig. 1, whose formulation is given by Eqs. (1-5). Initially, an intermittent contact situation is investigated, presenting trajectories, phase spaces, Poincare sections and frequency spectra for both the rotor and the stator. Besides, the time evolution of relative displacement, contact forces and SMA temperature attest the intermittent contact condition. After that, bifurcation diagrams varying the rotating speed are obtained for different convective coefficients, enabling a pattern analysis (chaotic *versus* periodic or quasi-periodic).

All results presented in this paper are based on the parameters shown in Tab. 1. According to these parameters, the linearized rotor natural frequency is $\omega_n \cong 140$ rad/s.

Table 1. Rotor system parameters.

Rotor					Gap	Stator			
m_r [kg]	k_r [kN/m]	c_r [Ns/m]	e [m]	r_r [m]	γ [m]	μ [-]	m_s [kg]	k_s [kN/m]	c_s [Ns/m]
50	980	280	0,001	0,1	0,006	0,1	50	14.580	2.700

SMA Layer									
A [$Nm^{-1}°C^{-1}$]	B [Nm^{-3}]	C [$Nm^{-5}°C$]	T_A [°C]	T_M [°C]	T_{amb} [°C]	c_l [$Jkg^{-1}°C^{-1}$]	m_l [kg]	A_l [m^2]	λ [-]
$1{,}3 \times 10^6$	$3{,}1 \times 10^{11}$	$2{,}0 \times 10^{16}$	40	14	25	400	1,0	0,2	0,5

The SMA behavior is presented in Fig. 2. For small displacement values, i.e. $\delta < 1$ mm, the SMA behavior for a "low" temperature (25 °C) looks like an elastic material with "low" stiffness (10.000 kN/m). Analogously, the same is valid for "intermediate" (50 °C – 50.000 kN/m) and "high" temperatures (100 °C – 100.000 kN/m).

As pointed out earlier, the SMA temperature is a consequence of two competing effects: the contact forces (friction heating) and the interaction with the surrounding environment (convection cooling). Both contact forces (normal and tangential) depend upon the SMA stiffness that, in turn, depends upon the SMA temperature; therefore, the system takes time to reach stabilized values for the pertinent variables. For this reason, the dynamical system response should be evaluated in steady state condition, neglecting the transient (stabilizing) period.

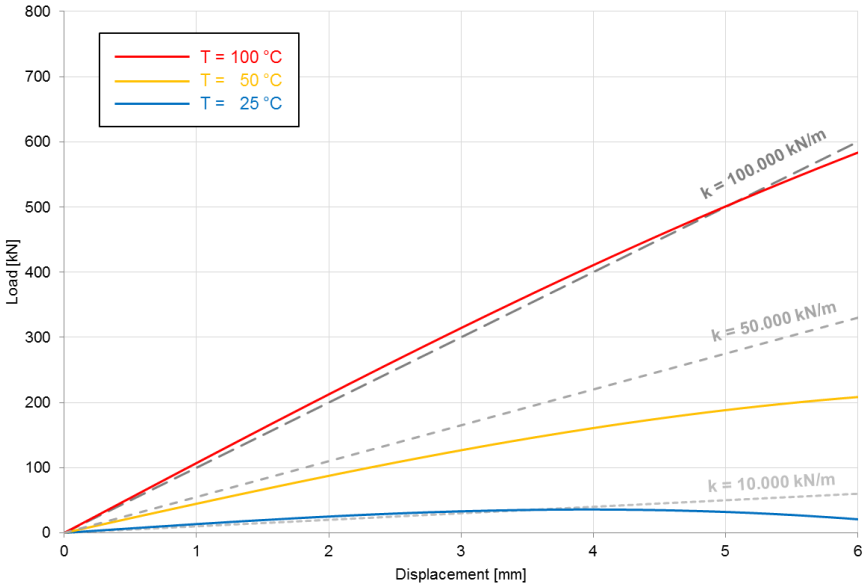

Figure 2. SMA coating behavior.

Figure 3 shows the first analysis conducted for Ω = 141,4 rad/s and h = 50 W/m^{2}K. The rotor displacement path for steady state regime, shown in Fig. 3a, presents a typical circular path for rotor systems. The phase space for x-direction displacement is presented in Fig. 3b together with the Poincare section that indicates a period-1 motion. This periodicity is attested by a predominant discrete peak in the frequency spectrum presented in Fig. 3c. Results associated to y-direction displacement are omitted, since their qualitative responses are the same as those obtained for x-direction.

Stator displacement path is shown in Fig. 3d and presents an irregular shape. Furthermore, it is noticeable that the orbits do not follow a single path. Despite the fact that there is no closed orbit in Fig. 3a, this response suggests kind of a pattern path. Nevertheless, the strange attractor depicted in the phase space of Fig. 3e together with the spread frequency spectrum shown in Fig. 3f indicate a chaotic behavior for the stator. Again, the y-direction results are similar to the x-direction ones and, therefore, they are omitted.

Rotor-stator relative displacement modulus is shown in Fig. 3g. Since the displacement behavior oscillates from values below and over the gap γ, it can be inferred that the system is subjected to intermittent contact. As a consequence from this condition, the contact forces (Fig. 3h) are also intermittent and alternate between zero and maximum value peaks. Since the adopted friction coefficient is μ = 0,1, the tangential force values are one tenth of the normal force magnitude, at all times. The tangential contact force is responsible for increasing the SMA layer temperature, as shown in Fig. 3i. The SMA temperature stabilizes after 200 s of time evolution and reaches approximately 100 °C. The SMA layer temperature stabilization implies a dynamical steady state response.

Results for relative displacement, contact forces and SMA temperature evolution are show in details for a short time interval from t = 249,9 s to t = 250,1 s in Figs. 3j – 3l. Shaded regions are associated, in Fig. 3j, to contact occurrence and, as a consequence, in Fig. 3k, to non-null contact forces. Therefore, it is noticeable from Fig. 3l that the shaded regions are associated with temperature increase. When there is no contact (unshaded regions), the relative displacement $|\underline{r}_{sr}|$ in Fig. 3j is lower than the gap γ = 0,006 m most of the time; thus, the contact forces in Fig. 3k are null and the temperature decreases (Fig. 3l), since only convection takes place with no friction.

The next analysis focuses on the convective coefficient influence on the system dynamics. Since stator dynamical response is much more complex than the rotor response, the first one is adopted for the analysis. Furthermore, x-direction is chosen instead of y-direction because the results are qualitatively equal. The results in Fig. 4 present bifurcation diagrams for stator displacement in x-direction as a function of the rotating speed for three different convective coefficients: h = 50 W/m^{2}K, h = 175 W/m^{2}K and h = 300 W/m^{2}K. The rotating speed is varied from Ω = 128 rad/s to Ω = 143 rad/s. All this range corresponds to intermittent contact conditions, as verified in preliminary simulations, out of the scope of this paper. It is noticeable that a much more complex behavior is associated to lower convective coefficients since, in general, the stable temperatures tends to be higher in such cases, leading to higher contact stiffness. Higher contact stiffness results on higher contact forces and, as a consequence, the discontinuity, which is the main nonlinearity in this dynamic system, becomes more prominent.

For the "low" convective coefficient h = 50 W/m^{2}K, the bifurcation diagram in Fig. 4a shows regions with high density of points – for instance: around Ω = 132 rad/s and from Ω = 138 rad/s to Ω = 142 rad/s. Outside these regions, the behavior is mostly periodic. As the convective coefficient increases to an "intermediate" value h = 175 W/m^{2}K, the periodic regions increase as the region with high density of points moves from the previous range to a new region defined by rotating speeds from Ω = 137 rad/s to Ω = 138 rad/s on the bifurcation diagram in Fig. 4b. Considering a "high" convective coefficient h = 300 W/m^{2}K, the bifurcation diagram in Fig. 4c becomes mostly periodic. In order to analyze such complex behaviors, the highlighted rotating speeds (dashed red lines) on the bifurcation diagrams are explored in details in Fig. 5, except for Ω = 141,4 rad/s in Fig. 4a (dashed blue line), which correspond to the previous analysis that has been already explored in Fig. 3.

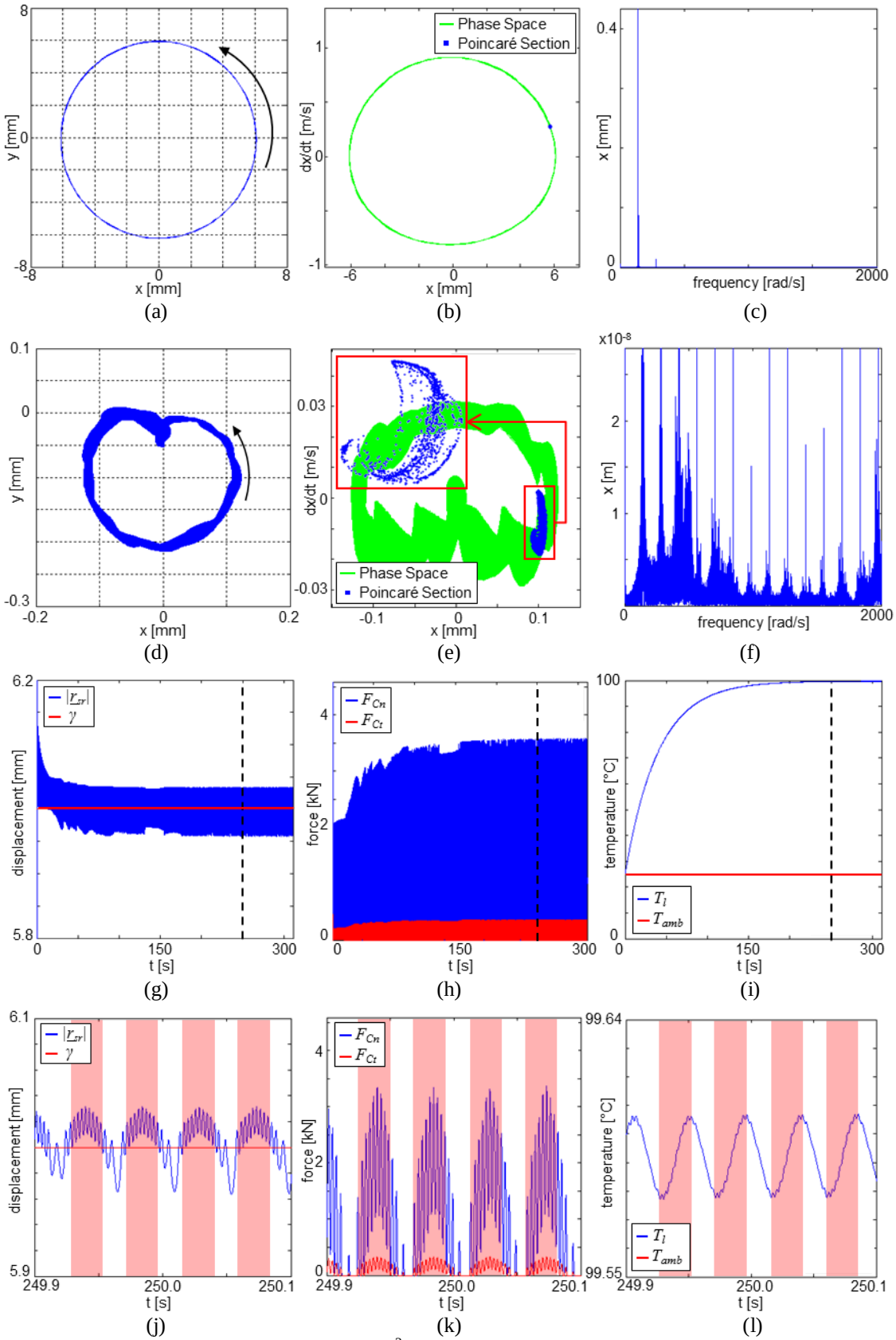

Figure 3. Results for Ω = 141,4 rad/s and h = 50 W/m^{2}K: (a) Rotor displacement path; (b) Rotor x-direction phase space orbits and Poincare section; (c) Rotor x-direction frequency spectrum; (d) Stator displacement path; (e) Stator x-direction phase space orbits and Poincare section; (f) Stator x-direction frequency spectrum; (g) Rotor-stator relative displacement time evolution; (h) Contact forces time evolution; (i) SMA layer temperature time evolution; (j) Rotor-stator relative displacement time evolution around t = 250 s; (k) Contact forces time evolution around t = 250 s and (l) SMA layer temperature time evolution at t = 250 s.

(a)

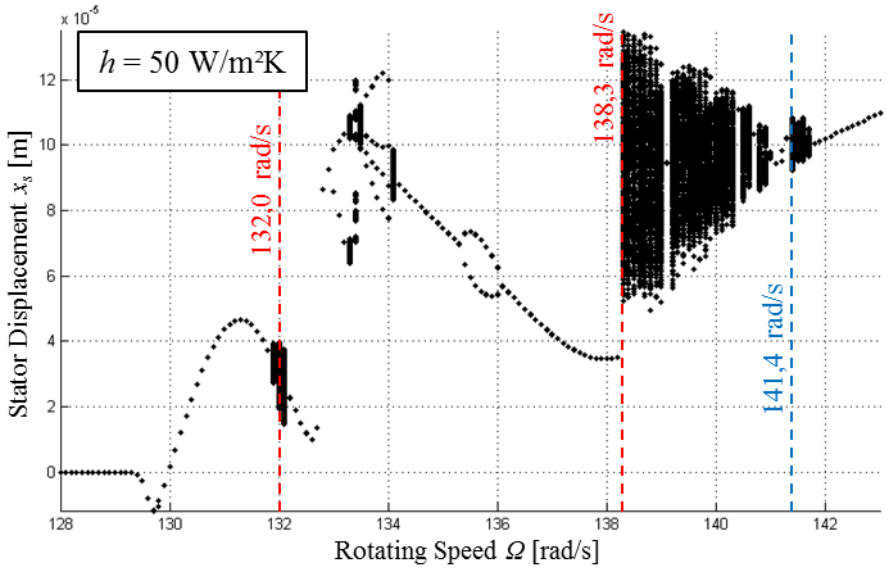

(b)

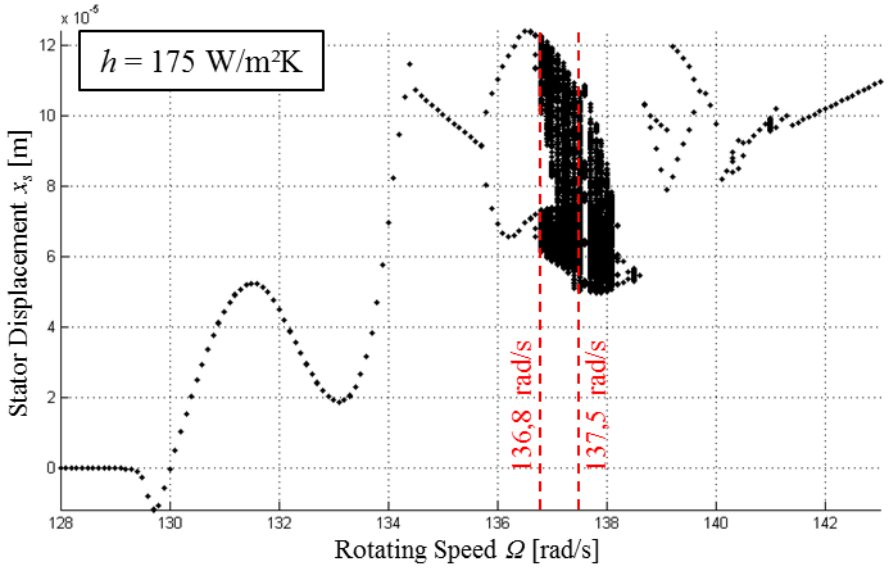

(c)

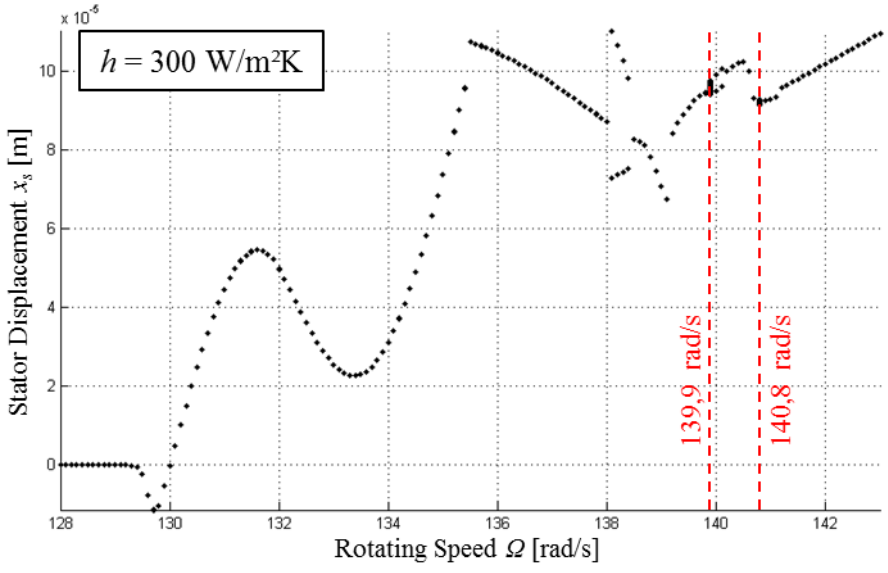

Figure 4. Bifurcation diagrams for different convective coefficients.
(a) 50 W/m^{2}K; (b) 175 W/m^{2}K and (c) 300 W/m^{2}K.

Regarding the low convective coefficient h = 50 W/m²K, the first highlighted rotating speed is Ω = 132 rad/s, which corresponds to the results shown in Fig. 5a. For this case, the Poincare section suggests a closed curve, which corresponds to a quasi-periodic behavior. The frequency spectrum shows well defined discrete peaks, characterizing this kind of behavior. Still considering h = 50 W/m²K, the second highlighted rotating speed is Ω = 138,3 rad/s and the corresponding results are shown in Fig. 5b. The Poincare section reveals a cloud of points and the frequency spectrum is spread, both characteristics of chaotic behavior.

Results related to the intermediate convective coefficient h = 175 W/m²K are associated to the highlighted rotating speeds Ω = 136,8 rad/s and Ω = 137,5 rad/s, whose results are shown on Figs. 5c and 5d, respectively. For the high convective coefficient h = 300 W/m²K, the highlighted rotating speeds are Ω = 139,9 rad/s and Ω = 140,8 rad/s and the results are shown in Figs. 5e and 5f, respectively. In all results from Figs. 5c to 5f, the presence of strange attractors as well as the spread frequency spectrum indicate chaotic behaviors.

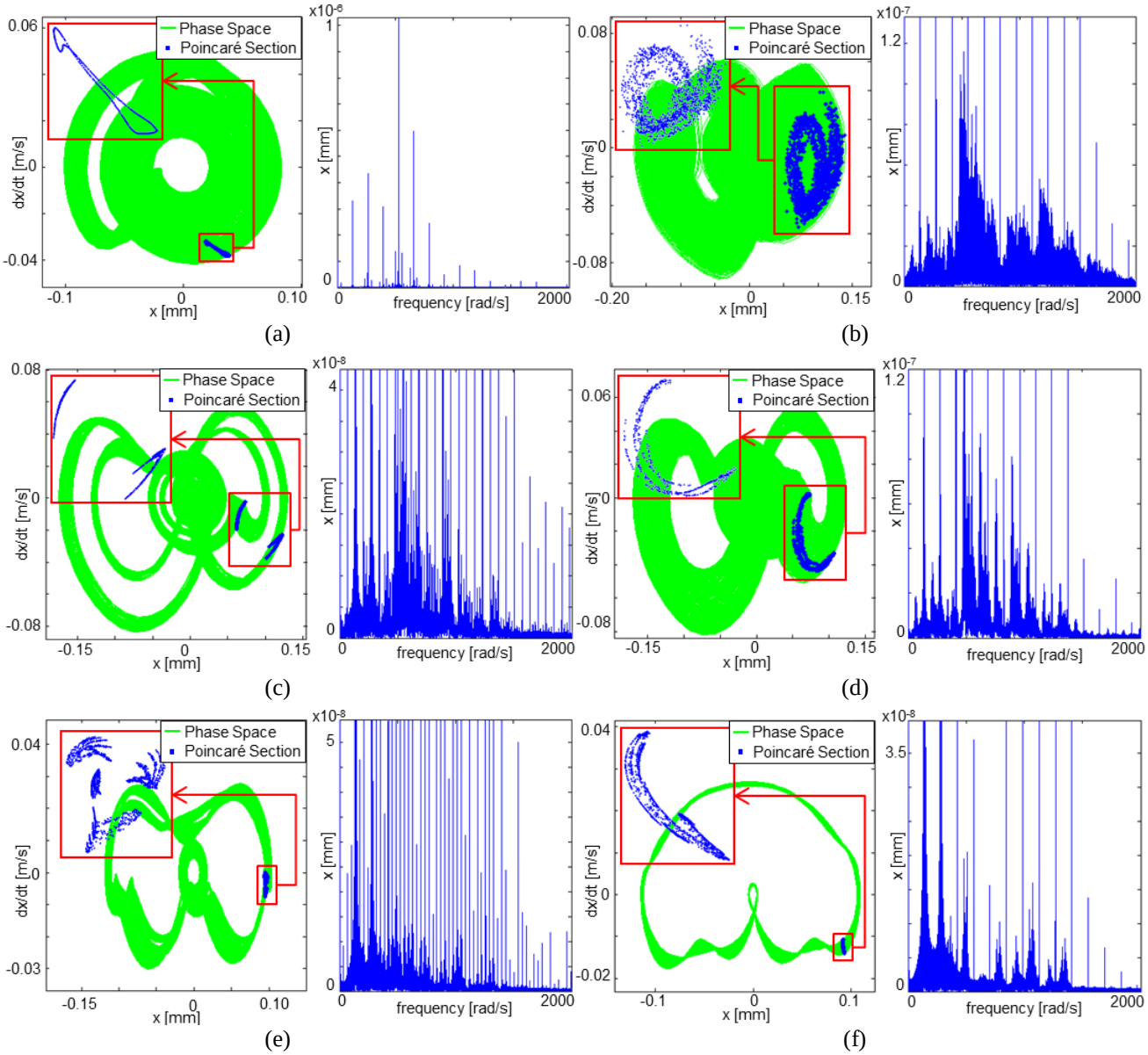

Figure 5 – Phase space, Poincare section and frequency spectrum results from rotating speeds highlighted in Fig. 4.

h = 50 W/m²K	
	Ω [rad/s]
(a)	132,0
(b)	138,3

h = 175 W/m²K	
	Ω [rad/s]
(c)	136,8
(d)	137,5

h = 300 W/m²K	
	Ω [rad/s]
(e)	139,9
(f)	140,8

4. CONCLUSIONS

The rotor dynamical model presented in this work considers intermittent contact and friction between rotor and stator through an SMA coating applied to the inner stator surface. Both the intermittent contact and the SMA layer behavior bring nonlinear characteristics to the system. As the SMA layer depends on the temperature, which is subjected to heating from friction and cooling from convection, a dynamic steady state condition is reached when the temperature stabilizes. Since the contact forces depend on the SMA behavior, the system dynamics is, at the same time, responsible for the SMA temperature variation and dependent on this own temperature (stiffness). Results show that a very complex dynamical response is associated to stator displacement, including chaotic responses. Characteristic strange attractors and spread frequency spectrums are presented and associated to such responses. Furthermore, the system response is evaluated when subjected to different convective coefficients. As lower convective coefficients are associated to higher SMA layer temperature and, therefore, higher contact stiffness, a more complex dynamic behavior is observed for such cases. On the other hand, lower convective coefficient values tend to reduce the responses complexity and even avoid chaos.

5. REFERENCES

Al-Beodoor, B. O. (2000) Transient Torsional and Lateral Vibrations of Unbalanced Rotors with Rotor-to-Stator Rubbing. Journal of Sound and Vibration 229(3), 627-645.

Bernardini, D. and Rega, G. (2010) The Influence of Model Parameters and of the Thermomechanical Coupling on the Behavior of Shape Memory Devices. International Journal of Nonlinear Mechanics. 45(10), 933–946.

Birman, V. (1996) Review of Constitutive Equations for Shape Memory Alloys. 11th ASCE Conference on Engineering Mechanics, New York, Vol. 2, 792-795.

Chávez, J.P., Wiercigroch, M. (2013) Bifurcation analysis of periodic orbits of a non-smooth Jeffcott rotor model. Communications in Nonlinear Science and Numerical Simulation 18, 2571-2580.

Choy, F.K., Padovan, J. (1987) Non-Linear Transient Analysis of rotor-Casing Rub Events. Journal of Sound and Vibration 113(3), 529-545.

Cisse, C., Zaki, W., Zineb, T. B. (2016). A Review of Constitutive Models and Modeling Techniques for Shape Memory Alloys. International Journal of Plasticity; Vol. 76; pp. 244–284.

Edwards, S., Lees, A. W., Friswell (1999) The influence of Torsion on Rotor/Stator Contact in Rotating Machinery. Journal of Sound and Vibration 225(4), 767-778.

Falk, F. (1980) Model Free-Energy, Mechanics and Thermodynamics of Shape Memory Alloys. ACTA Metallurgica, Vol.28, 1773-1780.

Falk, F. (1983) One-Dimensional Model of Shape Memory Alloys. Archives of Mechanics 35, 63-84.

Fonseca, C.A.L.L., Aguiar, R.R., Weber, H.I. (2016) On the Non-Linear Behaviour and Orbit Patterns of Rotor/Stator Contact with a Non-Conventional Containment Bearing. International Journal of Mechanical Sciences 105, 117-125.

Jeffcott, H.H. (1919) The Lateral Vibration of Loaded Shafts in the Neighbourhood of a Whirling Speed: The Effect of Want of Balance. Philosophical Magazine 37, 304-315.

Lagoudas, D.C. (2008) Shape Memory Alloys Modeling and Engineering Applications. Ed. Springer; 435 pp.

Lahriri, S., Santos, I. F. (2013) Theoretical Modelling, Analysis and Validation of the Shaft Motion and Dynamic Forces During Rotor-Stator Contact. Journal of Sound and Vibration, 332, 6359-6376.

Muszynska, A., Goldman, P. (1995) Chaotic Responses of Unbalanced Rotor/Bearing/Stator Systems with Looseness or Rubs. Chaos, Solitons and Fractals Vol. 5, No 9, 1683-1704.

Paiva, A., Savi, M. A. (2006) An Overview of Constitutive Models for Shape Memory Alloys. Mathematical Problems in Engineering; Article Id. 56876, Vol. 2006; 30 pp.

Popprath, S., Ecker, H. (2007) Nonlinear Dynamics of a Rotor Contacting an Elastically Suspended Stator. Journal of Sound and Vibration 308, 767-784.

Rankine, W.J.M. (1869) On the Centrifugal Force of Rotating Shafts. The Engineer 27, 249-249.

Santos, B.C., Savi, M. A. (2009) Nonlinear Dynamics of a Nonsmooth Shape Memory Alloy Oscillator. Chaos, Solitons and Fractals 40(1), 197–209.

Savi, M.A. (2015) Nonlinear Dynamics and Chaos in Shape Memory Alloy Systems. International Journal of Non-Linear Mechanics. 70, 2–19.

Silva, L.C., Savi, M. A., Paiva, A. (2013) Nonlinear Dynamics of a Rotordynamic Nonsmooth Shape Memory Allow System. Journal of Sound and Vibration 332, 608-621.

Sitnikova, E., Pavlovskaia, E., Wiercigroch, M., Savi, M. A. (2010) Vibration Reduction of the Impact System by an SMA Restraint: Numerical Analysis. International Journal of Nonlinear Mechanics 45(9), 837–849.

Varney, P., Green, I. (2015) Nonlinear Phenomena, Bifurcations, and Routes to Chaos in an Asymmetrically Supported Rotor–Stator Contact System. Journal of Sound and Vibration, 336, 207-226.

6. RESPOSIBILITY NOTICE

The authors are the only responsible for the printed material included in this paper.